Investigation of Human Low-Density Lipoprotein by ^{1}H Nuclear Magnetic Resonance Spectroscopy: Mobility of Phosphatidylcholine and Sphingomyelin Headgroups Characterizes the Surface Layer†

Helena C. Murphy,*,‡ Shamus P. Burns,‡ John J. White,‡ Jimmy D. Bell,§ and Richard A. Iles‡

Unit of Cell Regulation, Department of Diabetes and Metabolic Medicine, St. Bartholomew's and The Royal London School of Medicine and Dentistry, London E1 1BB, United Kingdom, and Robert Steiner NMR Unit, MRC Clinical Sciences Centre, Hammersmith Hospital, Imperial College School of Medicine, London W12 0HS, United Kingdom

Received January 4, 2000; Revised Manuscript Received April 28, 2000

ABSTRACT: The resolution of the trimethyl headgroup resonance of phosphatidylcholine (PC) and sphingomyelin (SM) in the intact human low-density lipoprotein (LDL) ^{1}H NMR spectrum at 600 MHz enabled the investigation of LDL surface structure and phospholipid-apoB interactions. We have previously shown that a higher proportion of PC headgroups (25−35% of total PC in LDL) compared to SM were tightly bound to apoB and therefore NMR-invisible [Murphy, H. C., et al. (1997) *Biochem. Biophys. Res. Commun. 234* (3), 733−737]. In the present study, we have investigated the mobility of phospholipid (PL) headgroups, using ^{1}H NMR spin−spin (T_2) relaxation measurements, in LDL isolated from nine volunteers. We show that both PC and SM exist in two additional and distinct environments indicated by the biexponential behavior of the relaxation decays in each case. The data showed that 36% of PC headgroups had a short T_2 component, mean T_2 of 31 ms, and 64% had a longer T_2 component of 54 ms. Approximately 15% of SM headgroups had a short T_2 component (mean T_2 of 27 ms) and 85% had a longer T_2 component of 78 ms. Therefore the majority of SM headgroups (85%) were more mobile than PC ($P < 0.001$) and since PC headgroups in organic media were more mobile than SM, we conclude that the characteristic high mobility of LDL SM is not an intrinsic property but arises from a high degree of order in molecular packing of the surface PL of human LDL. We suggest that because PC and SM interact differentially with cholesterol and possibly with neighboring phospholipids, this results in the formation of relatively long-lived microdomains of PL in vivo.

Low-density lipoprotein (LDL)[1] is the principal transporter of cholesterol in the circulation and high plasma LDL−cholesterol concentration is an independent risk factor for coronary heart disease (CHD) (*1*). The precise mechanism(s) by which LDL-derived cholesterol accumulates within cells and in the extracellular space of arterial walls, progressing to atherosclerotic lesions, is unclear, though a number of possibilities have been investigated: LDL fusion (*2*) and/or aggregation (*3*) and selective retention of LDL within the arterial intima, compared to non-apolipoprotein B containing lipoproteins (*4*). Increased retention of LDL could reflect its inherent size, (phospho)lipid composition, ability to bind vessel wall extracellular connective tissue components (*5*−*8*), and susceptibility to aggregation and fusion. Several lines of evidence suggest that oxidatively modified LDL plays an important role in the development of atherosclerosis (*1*, *9*, *10*). Oxidized LDL is rapidly taken up by macrophages leading to the formation of lipid-rich cells (foam cells), which contribute to the lipid-rich lesion core (*11*). Epidemiological studies have shown a strong positive correlation between saturated fatty acid intake, high serum cholesterol, and mortality from CHD (*12*). High intakes of saturated fat have been shown to raise plasma LDL−cholesterol levels while (poly)unsaturated ($n - 6$) fatty acids have an LDL-decreasing effect (*13*). Diet-induced alterations in lipoprotein metabolism may therefore contribute to possible pathological mechanisms.

LDL is composed of a hydrophobic core of neutral lipids, cholesteryl esters (CE), and triglycerides (TG), surrounded by a monolayer of hydrophilic phospholipids (PL), mainly sphingomyelin (SM) (25%) and phosphatidylcholine (PC) (66%), presenting an *N*-trimethyl headgroup to the surrounding (aqueous) environment. The large apolipoprotein B-100 (apoB) molecule covers approximately 30% of the particle surface and is thought to extend partly into the core. The normal physiological role of LDL to deliver cholesterol to peripheral cells via the receptor-mediated pathway is dependent upon the recognition of apoB by the LDL receptor. Evidence has accumulated that changes in lipid composition and mobility of cell membranes can influence the ability of the LDL receptor to bind LDL (*14*). Similarly, there is increasing evidence that the lipid composition of LDL has a

† We acknowledge the Ministry of Agriculture, Fisheries and Food (MAFF, U.K.) for funding the research.

* Address correspondence to this author: e-mail H.C.Murphy@mds.qmw.ac.uk; Fax 020 7377 7636.

‡ St. Bartholomew's and The Royal London School of Medicine and Dentistry.

§ Hammersmith Hospital, Imperial College School of Medicine.

[1] Abbreviations: NMR, nuclear magnetic resonance; LDL, low-density lipoprotein; PL, phospholipids; PC, phosphatidylcholine; SM, sphingomyelin.

10.1021/bi0000115 CCC: $19.00 © 2000 American Chemical Society
Published on Web 07/20/2000

fundamental role in the dynamic interaction with cell membranes, perhaps by modulating the conformation of apoB. Although LDL composition is known, the (phospho)-lipid−lipid and (phospho)lipid−protein interactions and the molecular organization of LDL are not well characterized. The surface PL conformation and organization may influence a number of the proposed pathological mechanisms, including fusion, aggregation, and susceptibility to oxidative damage. A better understanding of the structural organization and physicochemical properties at the LDL surface may therefore contribute to knowledge of the pathophysiological functions of LDL.

Study of the properties of lipoproteins has in part been limited by the need for a technique that does not perturb the structure. High-resolution NMR spectroscopy is noninvasive (and nondestructive) and has been used to study lipoproteins in intact plasma and isolated lipoproteins, yielding valuable information on lipid composition, molecular motion and structure (*15*, *16*). A ^{1}H NMR spectrum of LDL consists mainly of overlapping lipid signals with a narrow peak at 3.25 ppm arising from the methyl headgroups of PL. Using ^{1}H NMR spectroscopy at 600 MHz, we have previously demonstrated that the two main types of PL in LDL, PC and SM, can be resolved in the intact LDL spectrum (*17*). The PC and SM peak areas were obtained by Lorentzian line-shape analysis and a ratio of PC/SM was calculated for the intact LDL and lipid extract spectra. The difference between these two ratios revealed that approximately 20% of the total PL pool was immobilized and thus not visible in the intact LDL spectrum. This corresponded to 24% of the PC pool being immobilized, although the possibility that a small fraction of SM was also immobilized could not be entirely ruled out. The immobilization was attributed to tight interactions with apoB. Further evidence was provided by trypsinization of LDL, resulting in an increase of visible PC headgroups in the ^{1}H NMR spectrum.

The resolution of PC and SM in the ^{1}H NMR spectrum of intact LDL has provided the opportunity to investigate the environments of each PL without disruption of the LDL structure. The work presented in this study is based upon a property of ^{1}H (proton) NMR spectroscopy, namely, spin−spin (T_2) relaxation, which can provide detail concerning the molecular motion of specific moieties within LDL (*15*). Nuclei exhibit different rates of relaxation dependent on factors such as the surrounding environment and strengths of intermolecular interactions. We report and discuss our findings obtained from T_2 relaxation studies of PC and SM in LDL isolated from normolipidemic volunteers, which further characterizes the surface structure of human LDL.

MATERIALS AND METHODS

Isolation of LDL. Volunteers were recruited from academic departments within St. Bartholomew's and the Royal London Hospital School of Medicine and Dentistry. Nine healthy males (volunteers A−I), ranging from 30 to 56 years of age (mean ± SEM 41.4 ± 2.9 years), who had no known family history of coronary heart disease took part in the study. None were taking drugs known to affect lipid metabolism. Venous blood was collected from the volunteers' brachial vein after an overnight fast. Several blood samples were taken from each volunteer over a period of 2 years. Plasma total cholesterol, HDL−cholesterol, and triglyceride concentrations were measured for each of the volunteers and LDL−cholesterol levels were calculated by use of the Friedewald approximation (*18*). All volunteers were normolipidemic: total cholesterol ranged from 3.5 to 5.4 mmol·L^{-1}; triglycerides, 0.65−1.59 mmol·L^{-1}; HDL−cholesterol, 1.03−2.05 mmol·L^{-1} and LDL−cholesterol, 1.7−3.46 mmol·L^{-1}. Blood collected for LDL isolation (40−45 mL) was immediately placed into tubes containing 1 mg·mL^{-1} whole blood of EDTA disodium salt (Na_2EDTA, Sigma, U.K.) and 0.1 mg·mL^{-1} sodium azide (NaN_3). Tubes were left to stand for approximately 30 min at 4 °C and then centrifuged at 900*g* for 20 min at 4 °C. The plasma was then aspirated and stored at 4 °C until LDL isolation within 1 h.

The plasma density was adjusted to 1.3 g·mL^{-1} by the addition of sodium bromide and then underlaid (up to ∼ 4 mL) in 30 mL capacity centrifuge tubes containing 0.9% saline solution. The tubes were then centrifuged at 40 000 rpm for 3 h in a Sorvall ultracentrifuge using a fixed-angle T-865 Sorvall rotor (Du Pont, Sorvall, U.K.). The crude LDL fraction at a density of 1.025−1.055 g·mL^{-1} was removed and placed in a second ultracentrifuge tube containing 5 mL of 18% NaBr solution and topped up with 8% NaBr solution and recentrifuged for 17 h at 40 000 rpm. All solutions used during the isolation procedure contained 37.2 mg·L^{-1} Na_2-EDTA and 0.1 g·L^{-1} NaN_3. All reagents used were of analytical grade (BDH, U.K.) unless otherwise stated. The washed LDL at the top of the tube was removed by aspiration and stored at 4 °C until dialysis (usually within 1 h). In total, 50 LDL samples were isolated from the nine volunteers.

Preparation of Samples for NMR Spectroscopy: (a) Intact LDL. LDL samples were dialyzed in Centricon-100 diafiltration tubes, MW cutoff 50 kDa (Amicon, U.K.), against deuterated phosphate-buffered saline (99% ^2H_2O) containing 10 mM sodium phosphate, 0.137 M NaCl, 2.7 mM KCl, and 10 mM Na_2EDTA, p^{2}H 7.0. All deuterated solvents were purchased from Aldrich Chemical Co, Dorset, U.K. The concentration of the dialyzed LDL was determined by Peterson's modification of the Lowry procedure (*19*, *20*) (Sigma Diagnostics, Sigma, Poole, U.K.) and adjusted to 1.67 mg of protein·mL^{-1}. The LDL fraction was stored at 4 °C and the NMR measurements were performed within 1 week. The LDL samples were transferred to 5 mm (outer diameter) tubes and sodium trimethylsilyl[2,2,3,3-$^2H_4$]propionate (TSP-d_4) was added as an internal chemical shift standard (final TSP-d_4 concentration 2 mM). The final LDL concentration in the NMR samples was 1.5 mg of protein·mL^{-1}.

(b) Standard Solution of PC and SM. A standard solution of PC and SM (egg yolk PC and bovine brain SM, Sigma, U.K.) was made up in the same proportions as those found in LDL (PC/SM ratio of 2.33) in 2:1 C^2HCl_3/$C^2H_3O^2H$ and transferred to a 5 mm NMR tube with 2 mM tetramethylsilane (TMS) as the chemical shift reference. The sample was stored at −70 °C until NMR analysis.

^{1}H NMR Spectroscopy: (a) Intact LDL. ^{1}H NMR spectroscopy of the intact LDL samples was performed at 600 MHz using a Bruker AMX spectrometer. The 90° and 180° pulse widths were calibrated and spin−spin (T_2) relaxation measurements were performed with the Carr−Purcell−Meiboom−Gill (CPMG) sequence, $[90°_x - \tau - 180°_y - \tau$-(echo) $- \tau - 180°_y - \tau$(echo) $- \tau$...$180°_y - \tau$(echo) $-$ acq$]_n$, where $2n\tau$ was 0.5 ms. Thirty-six τ increments with total

echo times of 2−500 ms were obtained. During the CPMG experiment the samples were maintained at 310.3 K (37.3 °C), nonspinning, 16 scans and 16K data points per FID. The NMR probe temperature was calibrated by a standard technique (*21*), by use of a thermocouple and the chemical shift of ethylene glycol vs temperature, which has an approximately linear relationship between 20 and 50 °C). This method provided data that were fit to a straight line, the statistics of the fit providing data on temperature variability within the probe. The calibration curve showed that when the probe temperature was set to 310 K the actual temperature was 310.3 ± 0.4 K.

(b) Standard Solution of PC and SM. The spin−spin (T_2) relaxation experiment was performed at 600 MHz with the CPMG sequence after calibration of the 90° and 180° pulse widths. Thirty-eight τ increments (total echo times of 2−2000 ms) were used, with a $2n\tau$ value of 0.05 s. During the CPMG experiment the samples were maintained at 298 K, nonspinning, 16 scans and 16k data points per FID.

Analysis of NMR Spectra. Line shape fitting analysis was applied to resolve the areas of the phospholipid $N(CH_3)_3$ resonances in the ^{1}H NMR spectra. Program FITPLA^C using Lorentzian line shapes was used (*17*). The frequency regions of the phospholipid peak were analyzed in each of the spectra obtained at the time points (τ increments) in order to calculate the relaxation decay rates (T_2) of the PC and SM choline headgroup. The first 25 spectra (2−200 ms) obtained from the CPMG experiment of intact LDL were analyzed, since in spectra obtained where τ values were greater than 200 ms, most of the NMR signals had decayed and the signal/noise (S/N) ratio was therefore too low to fit Lorentzian components. However, even in spectra obtained at the longer τ values up to 200 ms the reliability of the fitting procedure declined, so to overcome this problem, line shape analysis was performed with the half-height line widths at each successive τ increment fixed to that obtained at the first τ increment. The S/N ratio was not a problem for the standard PC/SM solution in organic media and therefore all 38 spectra obtained from the CPMG experiment were analyzed.

Data Analysis and Statistics. The PC and SM peak areas obtained from the Lorentzian line shape analyses were plotted against τ (milliseconds). Exponential curves were fitted using the Levenburg-Marquardt algorithm (*22*) to obtain the T_2 relaxation decay rates (time constants). The curves fitted were either monoexponential or biexponential (Program Table Curve 2D; Jandel Scientific, Germany). The best fit was determined by the F statistic. This is a measure to which the given equation represents the data, based on the minimum residual sum of squares, and taking into account the number of parameters used in the fit, such that increasing the parameter count does not necessarily improve the significance of the fit.

RESULTS

(a) Intact LDL. A typical ^{1}H NMR spectrum of intact LDL from one of the nine volunteers (volunteer B) at 37.3 °C is shown in Figure 1. The spectrum consists of relatively broad resonances arising from triglycerides (TG), phospholipids (PL), unesterified cholesterol, and cholesteryl esters. Peak 9 arises from the $N^+(CH_3)_3$ (3.25 ppm) of the PL *N*-trimethyl choline headgroups (other assignments are given in the figure legend). It can be seen that this resonance is resolved into two components at 600 MHz (Figure 1b), which we have previously assigned to phosphatidylcholine (PC) at 3.25 ppm and sphingomyelin (SM) at 3.24 ppm, respectively (*17*).

Figure 2 shows a stacked plot of sequential spectra from the PL region in intact LDL (volunteer G) from the T_2 CPMG experiment. It is clear that the rate of decline of the PC signal at 3.25 ppm is greater than that of SM at 3.24 ppm. This is confirmed by analyzing each spectrum at the given τ value by Lorentzian line shape fitting to resolve the areas of the two overlapping resonances.

Figure 3 shows the exponential decay of the peak areas of PC and SM (volunteer D). The best-fit exponential curves (to obtain the relaxation decay time constants, T_2) were biexponential and the resulting T_2 values for PC and SM are given. Based on the F statistic and the regression coefficient, the best-fit curve in the majority of cases was biexponential. Of the 50 intact LDL T_2 experiments carried out, 41 (82%) and 47 (94%) were significantly biexponential for PC and SM T_2 relaxation decay, respectively.

The biexponential curves fitted to the experimental data produced parameters describing two relaxing T_2 components: a slow-relaxing component and a fast-relaxing component. Biexponential spin−spin relaxation can be described by:

$$M(t) = M_s \exp(-t/T_{2s}) + M_l \exp(-t/T_{2l})$$

where $M(t)$ is the total magnetization decaying with echo time t. M_s and M_l are the equilibrium magnetizations of the slow and fast relaxing components and T_{2s} and T_{2l} are their spin−spin relaxation time constants. The parameters M_s and M_l represent the fractional contribution to the time constants T_{2s} and T_{2l}, respectively, and t is the τ increment (milliseconds). Hereafter, the T_2 values are called the short T_2 (T_{2s}) and long T_2 (T_{2l}) and the parameters M_s and M_l are referred to as the fraction of short T_2 (fT_{2s}) and fraction of long T_2 (fT_{2l}), respectively.

Tables 1 and 2 show the T_2 data obtained for PC and SM headgroups, respectively, in intact LDL isolated from nine volunteers (A−I). LDL was isolated from each volunteer several times over a period of 2 years (as shown by the n numbers) and T_2 measurements were obtained for each sample (mean ± SEM). Table 1 shows that approximately 36% of PC headgroups had a short T_2 component, mean T_{2s} of 31 ms, and 64% had a longer T_2 component (T_{2l}) of 54 ms. Table 2 shows that 15% of SM headgroups had a short T_2 component (mean T_{2s} of 27 ms) and 85% had a longer T_2 (T_{2l}) component of 78 ms. The 85% of SM headgroups that had the long T_2 were significantly more mobile than all PC headgroups ($P < 0.001$, unpaired t-test).

Analysis of variance (one-way ANOVA) was carried out to assess subject intra- and intervariability of the T_2 values. The intra- and intervariabilities (coefficient of variation, CV) of PC T_{2s} were calculated as 20%. The intra-and intervariability CVs of PC T_{2l} were 9% and 11%, respectively. There were no significant differences between the volunteers for the T_2 values of PC headgroups. The intra- and intervariability CVs of SM T_{2s} were calculated as 25% and 35%, respectively, and the intra-and intervariability CVs of SM T_{2l} were 5% and 9%, respectively. The SM T_{2l} of volunteer

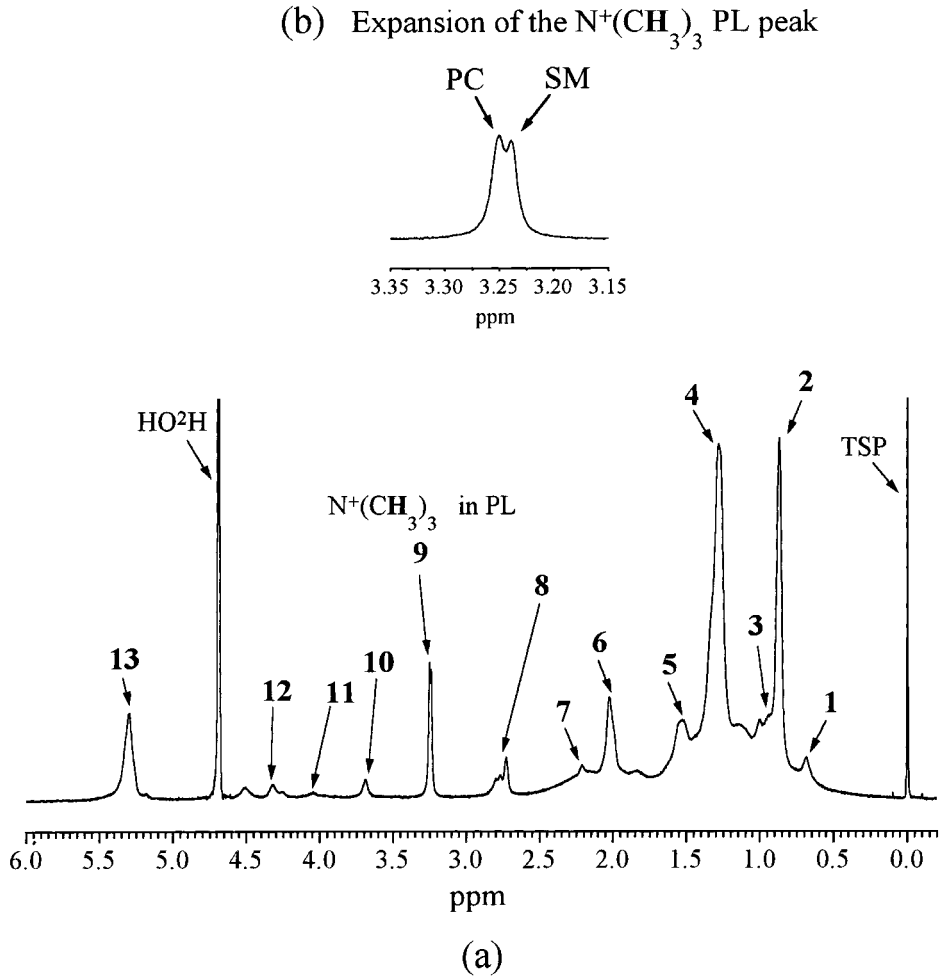

FIGURE 1: Typical ^{1}H NMR spectrum of intact LDL (volunteer B) at 37.3 °C. The labeled peaks in the spectrum are assigned to (1) C(18)H_3 (0.65 ppm) from total cholesterol; (2) CH_3 (0.89 ppm) from fatty acyl chain termini; (3) C(19 and 21)H_3 (0.94 ppm) from total cholesterol; (4) (CH_2)$_n$- (1.28 ppm) from the fatty acyl chain backbone; (5) CH_2CH$_2$CO (1.53 ppm) from the fatty acyl chains; (6) CH_2−CH═CH− (2.02 ppm) from the monounsaturated fatty acyl components; (7) CH_2CO (2.21 ppm) from the fatty acyl chains; (8) −CH═CH−CH_2−CH═CH− (2.8 ppm) from polyunsaturated fatty acyl components; (9) N$^+$(CH_3)$_3$ (3.25 ppm) from the PL *N*-trimethyl choline headgroups; (10) CH_2N$^+$(CH$_3$)$_3$ (3.68 ppm) in PL; (11) C(3)H_2O (4.04 ppm) from the glycerol backbone in PC; (12) CH_2CH$_2$N$^+$(CH$_3$)$_3$ (4.32 ppm) in PL; (13) −*H*C═C*H*− (5.34 ppm) from the double-bond protons found in all unsaturated fatty acyl moieties. PL, phospholipids; PC, phosphatidylcholine; TG, triglycerides. Assignments are based on those of Hamilton et al. (*15*). Panel b is an expansion (3.15−3.35 ppm) of the N$^+$(CH_3)$_3$ region showing the resolution of phosphatidylcholine (PC) and sphingomyelin (SM) resonances.

A differed significantly (Tukey-HSD test, $P < 0.05$) from volunteers B and G only. Replicate analyses of an LDL sample isolated from volunteer B was carried out to assess the repeatability of the T_2 experiment and showed that the variation was similar to that resulting from individual measurements made over the 2 year period. For SM, the fT_{2s} was 0.16 ± 0.05; T_{2s}, 43.9 ± 5.93 ms; fT_{2l}, 0.84 ± 0.05; and T_{2l}, 91.41± 1.94 ms. For PC, the fT_{2s} was 0.38 ± 0.10; T_{2s}, 40.43 ± 2.55 ms; fT_{2l}, 0.62 ± 0.10; and T_{2l}, 61.8 ± 1.8 ms [mean (n = 3) ± SEM].

(b) Standard Solution of PC and SM. A stacked plot of sequential spectra from the standard PL T_2 experiment is shown in Figure 4. Based on the *F* statistic and the regression coefficient, the best-fit curves were monoexponential. The T_2 values calculated for PC and SM were 577 and 533 ms, respectively. The monoexponential curves for PC and SM generated from the Lorentzian line shape analysis of these data are shown in Figure 5. In organic solvent (C^{2}HCl$_3$/C^{2}H$_3$O^{2}H, 2:1), the mobility of the PL headgroups increased considerably (approximately 10-fold), and in contrast to intact LDL, the PC headgroups had a longer T_2 value than SM.

DISCUSSION

We have demonstrated that phosphatidylcholine (PC) and sphingomyelin (SM) methyl headgroups within the LDL surface exist in distinct (micro)environments. The majority of SM (85%) resides within a distinctly more mobile phospholipid (PL) pool than that of both PC components, with the remaining fraction being far less mobile than PC. These data support a previous fluorescence study of LDL (*23*), which showed that 1,6-diphenyl-1,3,5-hexatrienylpropionyl- (DPH-) labeled SM molecules in LDL were more mobile than DPH-labeled PC. However, this present study with ^{1}H NMR spin−spin relaxation (T_2) measurements also suggests that both PC and SM headgroups exist in at least two distinct environments, indicated by the strongly biexponential behavior of the relaxation decays in each case. Studies of LDL phospholipid organization by ^{1}H, ^{2}H, ^{13}C, and ^{31}P NMR spectroscopy have also been reported previously (*24*−*27*). Finer et al. (*24*) observed the field dependence of the N$^+$(CH$_3$)$_3$ line widths in ^{1}H NMR studies of porcine LDL by making measurements at two magnetic field

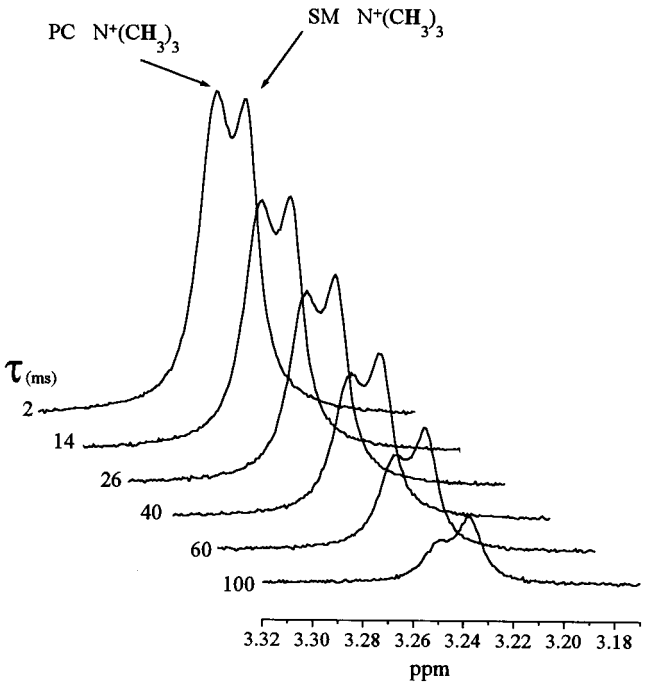

FIGURE 2: Stacked plot of sequential ^{1}H NMR spectra of the phospholipid region (3.17−3.32 ppm) from a T_2 experiment of intact LDL (volunteer G). Only six spectra from the CPMG experiment obtained at the τ increments on the left are shown for clarity.

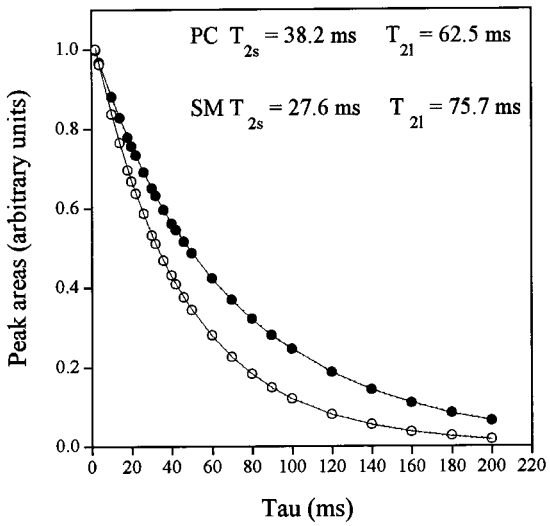

FIGURE 3: Exponential decay curves generated from the T_2 spectral data obtained from the ^{1}H NMR CPMG measurements of intact low-density lipoprotein (volunteer D). The phosphatidylcholine and sphingomyelin $N^+(CH_3)_3$ peak areas (normalized to 1.0) are plotted against τ [PC, (○) and SM (●)], together with the biexponential curves fitted (solid line) and the 95% confidence limits (dotted line). The T_2 values obtained from curve fitting are also shown, where T_{2s} and T_{2l} represent the short and long T_2 values, respectively.

strengths corresponding to ^{1}H resonance frequencies of 100 and 220 MHz and concluded that the choline headgroups are likely to be present in a range of different chemical environments. The ^{2}H NMR studies of Chana et al. (*25*) suggest two PL domains with different order parameters at the LDL (and VLDL) surface; however, they cannot be directly compared with our ^{1}H NMR findings since the ^{2}H probes are placed in the methylene groups of the fatty acyl chains describing molecular interactions of these deuterated -CH_2- groups at the hydrocarbon region of the surface. Furthermore, no previous ^{1}H NMR study has been capable

Table 1: T_2 Values of the *N*-Trimethyl Protons of Phosphatidylcholine (PC) in Intact LDL from Nine Volunteers[a]

volunteer	*n*	T_{2l} (ms)	fT_{2l}	T_{2s} (ms)	fT_{2s}
A	8 (7)	54.4 ± 0.5	0.65 ± 0.03	32.5 ± 0.9	0.35 ± 0.03
B	8 (7)	51.0 ± 1.1	0.75 ± 0.06	27.5 ± 2.1	0.25 ± 0.06
C	2 (2)	54.4	0.60	32.5	0.40
D	7 (6)	55.6 ± 2.3	0.57 ± 0.08	32.1 ± 2.2	0.43 ± 0.08
E	2 (2)	57.6	0.55	32.6	0.45
F	3 (2)	53.8	0.76	24.5	0.24
G	7 (4)	50.0 ± 1.0	0.71 ± 0.04	29.0 ± 1.3	0.29 ± 0.04
H	7 (6)	58.2 ± 2.3	0.54 ± 0.08	34.9 ± 3.0	0.46 ± 0.08
I	6 (5)	53.4 ± 2.0	0.67 ± 0.06	31.7 ± 2.6	0.33 ± 0.06
	mean[b]	54.3 ± 0.9	0.64 ± 0.03	30.8 ± 1.1	0.36 ± 0.03

[a] The T_2 values shown are mean ± SEM. In each case, a biexponential curve was fitted to the PC peak areas obtained from the ^{1}H NMR CPMG experiment, and thus two T_2 values were obtained; a long T_2 value (T_{2l}) and a short T_2 value (T_{2s}), with fT_{2l} and fT_{2s} representing the fractional contribution to the corresponding T_2 value (sum of fractions = 1.0). *n* represents the number of LDL measurements made from each volunteer over a period of 2 years and the numbers in parentheses are those that were significantly biexponential. [b] Mean of means from the nine volunteers.

Table 2: T_2 Values of the *N*-Trimethyl Protons of Sphingomyelin (SM) in Intact LDL from Nine Volunteers[a]

volunteer	*n*	T_{2l} (ms)	fT_{2l}	T_{2s} (ms)	fT_{2s}
A	8 (8)	82.7 ± 2.4	0.80 ± 0.04	32.6 ± 2.5	0.20 ± 0.04
B	8 (8)	75.6 ± 0.8	0.88 ± 0.01	25.0 ± 2.4	0.12 ± 0.01
C	2 (2)	80.3	0.77	29.8	0.23
D	7 (7)	77.1 ± 0.6	0.85 ± 0.02	27.6 ± 1.3	0.15 ± 0.02
E	2 (2)	76.6	0.89	25.7	0.11
F	3 (2)	79.1	0.87	27.3	0.13
G	7 (5)	73.5 ± 0.7	0.86 ± 0.01	24.8 ± 1.3	0.14 ± 0.01
H	7 (7)	76.7 ± 1.5	0.87 ± 0.02	21.7 ± 3.7	0.13 ± 0.02
I	6 (6)	76.0 ± 2.1	0.83 ± 0.03	25.2 ± 3.3	0.17 ± 0.03
	mean[b]	77.5 ± 0.9	0.85 ± 0.01	26.6 ± 1.1	0.15 ± 0.01

[a] The T_2 values shown are mean ± SEM. In each case, a biexponential curve was fitted to the SM peak areas obtained from the ^{1}H NMR CPMG experiment, and thus two T_2 values were obtained; a long T_2 value (T_{2l}) and a short T_2 value (T_{2s}), with fT_{2l} and fT_{2s} representing the fractional contribution to the corresponding T_2 value (sum of fractions = 1.0). *n* represents the number of LDL measurements made from each volunteer over a period of 2 years and the numbers in parentheses are those that were significantly biexponential. [b] Mean of means from the nine volunteers.

of distinguishing between PC and SM directly.

Of the 50 intact LDL T_2 experiments carried out, 41 (82%) and 47 (94%) were significantly biexponential for PC and SM, respectively. Five of the 12 nonsignificant biexponential fits arose from one volunteer (volunteer G), who showed no significant differences in blood lipids compared with the other volunteers (data not shown). While we cannot rule out that the NMR-determined poor biexponential behavior of LDL phospholipids has some biological significance, we believe that the cases of weak biexponential fit are most likely to arise from known difficulties in fitting multiexponential curves. Fitting has been shown to be most difficult when the two time constants describing the biexponential are not greatly different (*28*), and this would explain why the amplitude errors for the two T_2 values of PC are greater than for SM; the difference between the measured T_2 values for PC was smaller than for SM, increasing the difficulty of the fitting procedure. Clayden et al. (*28*) also showed that the S/N ratio is critical in determining confidence of biexponential data and suggested an ideal S/N ratio of at least 1000:1. In general, the S/N ratio in our experimental

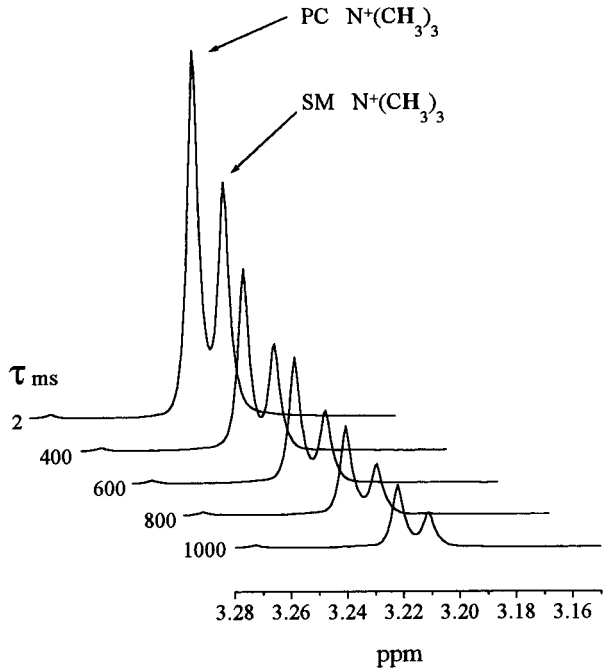

FIGURE 4: Stacked plot of sequential ^{1}H NMR spectra of the phospholipid region (3.15−3.28 ppm) from a T_2 experiment of a standard solution of PC and SM (PC/SM ratio of 2.33; egg yolk PC and bovine brain SM). Five spectra from the CPMG experiment obtained at the τ increments on the left are shown for clarity.

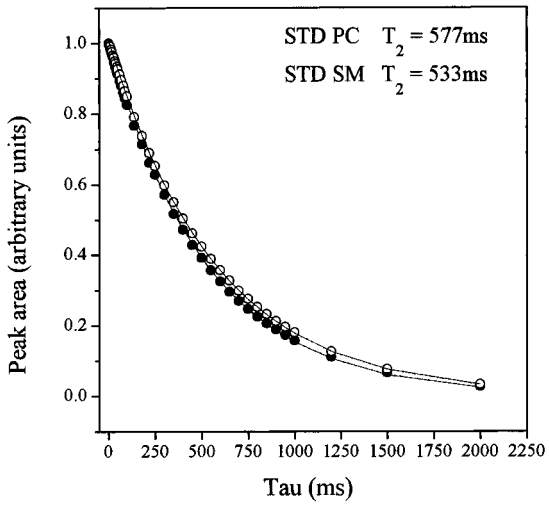

FIGURE 5: Exponential decay curves generated from the T_2 spectral data obtained from the ^{1}H NMR CPMG measurements of a standard solution of PC and SM (PC/SM ratio of 2.33; egg yolk PC and bovine brain SM). The phosphatidylcholine and sphingomyelin $N^+(CH_3)_3$ peak areas (normalized to 1.0) are plotted against τ [PC (○), and SM (●)], together with the monoexponential curves fitted (solid line) and the 95% confidence limits (dotted line). The T_2 values obtained from curve fitting are also shown.

data was between 300:1 and 200:1 at the first τ increment. The S/N ratio for the data shown in Figure 2 began at 234:1 but decreased to 39:1 at the longest τ. This is likely to be the cause of the majority of the variation in amplitudes (and T_2 values), and why a small number of LDL samples showed poor biexponential behavior. The T_2 values (especially T_{2l}) for each volunteer showed relatively little variation over the 2 years of collecting samples (approximately 5−10%). This study assessed the intra- and intersubject variation of LDL surface structure of volunteers on free-living diets, whereas most investigations of LDL structure have carried out experiments on pooled LDL samples isolated from several volunteers. The variability of T_2 values obtained from 50 LDL samples isolated from the same nine volunteers (over 2 years) is very similar to the variability obtained between volunteers. The data shows that there was little difference in PC and SM mobility between volunteers. There were no significant differences of the T_2 measurements between the volunteers, apart from the SM T_{2l} of volunteer A differing from those of volunteers B and G only. Though this difference might suggest biological variation and have structural/functional consequences for LDL, the magnitude of this difference is small (approximately 12%) and may simply represent the upper limit of the normal range of SM mobility. The intravariability of PC and SM T_2 values was fairly small (5−10% for T_{2l} and 20−25% for T_{2s}) suggesting that the surface characteristics of LDL are conserved, i.e., they remain similar over the 2-year period. We have carried out repeated T_2 experiments ($n = 3$) on one LDL sample, which showed that the variation was similar to that resulting from individual measurements made over the 2-year period. This suggests that the source of variation over time is not due to changes in LDL mobility but due to the errors associated with making T_2 measurements and curve-fitting.

The T_2 values of a standard solution of PC and SM in organic media ($C^2HCL_3/C^2H_3O^2H$ 2:1 mixture) were much longer than intact LDL and in this case showed that PC was slightly more mobile than SM. Previous NMR T_2 studies from this laboratory have shown that outer PL headgroup mobility in single unilamellar vesicles (SUVs) was greater if the SUVs were composed of PC rather than SM (114 ms compared with 25 ms, respectively; Murphy et al., unpublished data). Other work has also suggested that SM forms more condensed monolayers than equivalent PC monolayers in SUVs, in the absence of cholesterol (*23*, *29*−*31*). Sommer et al. (*23*) studied vesicle systems using fluorescence anisotropy measurements and showed that the DPH-labeled PC vesicle was more mobile than the equivalent DPH−SM vesicle. The DPH probe is located in the fatty acyl chain region of the PL vesicle bilayer and describes tighter packing of SM fatty acyl chains. The greater mobility of SM headgroups at the LDL surface is unlikely to arise from the intrinsic structural differences between the two phospholipids, but instead arises from the organized arrangement of surface (and perhaps core) lipids, the molecular packing of which may influence the size and mobility of the LDL particle.

Unesterified cholesterol, thought to be primarily located in the surface of the LDL, with perhaps a relatively small fraction situated in the core (*32*), may have a major influence on the molecular packing of LDL PL. The ^{13}C NMR studies by Lund-Katz and Phillips (*27*) using labeled [4-^{13}C]-cholesterol indicated that 70% of unesterified cholesterol resides in the surface and 30% within the core. Cholesterol molecules are thought to insert into a PL bilayer with the hydroxyl group oriented toward the polar headgroup and the hydrocarbon tail toward the hydrophobic core of the bilayer—the long axis of cholesterol is then oriented perpendicular to the bilayer plane. The β-hydroxyl group could then participate in H-bonding with the carbonyl oxygen, linking the PL fatty acyl chain with its glycerol backbone (*33*). The rigid sterol ring may form van der Waals interactions with adjacent fatty acyl chains inhibiting the formation of kinks (resulting from double bonds) and decreasing the number

of gauche conformations. Cholesterol incorporation may therefore have a condensing effect on acyl chains in the fluid state (*34*). When the PL are in the gel state, insertion of cholesterol might disrupt the intermolecular bonding in PL bilayers (*35*), causing increased separation between the headgroups, decreasing intermolecular (electrostatic) interactions between them (*34*). This may result in increased freedom of motion (i.e., mobility) of the headgroup, and is likely to be dependent on the type of PL [e.g., degree of (un)saturation and chain length]. For example, the studies by McIntosh et al. (*36*) showed that incorporation of cholesterol into bovine brain SM and *N*-tetracosanoylsphingomyelin (C24 SM) fluidized the bilayers and that an equimolar concentration of cholesterol converted the gel state to the liquid crystalline one.

It has previously been proposed that cholesterol may be the main modulator of lipid organization at the LDL surface (*25*). Chana et al. (*25*) suggested that the low-order (high-mobility) domain (less than 10%) in the LDL surface observed with ^{2}H probes in the fatty acyl chain of PL was a cholesterol-deficient region and conversely the high-order (low-mobility) domain was cholesterol-rich. However, these studies could not distinguish between the two main PL in LDL and their possible roles in modulating LDL surface mobility due to differential affinities for cholesterol. Interaction of unesterified cholesterol and PL in lipoproteins has been studied previously with ^{13}C-labeled cholesterol and NMR (*27*). The tighter packing of the PL/cholesterol monolayer in the surface of LDL, compared to HDL, was suggested to be due to the lower PC/SM ratio, the higher unesterified cholesterol/PL ratio, and the greater acyl chain saturation of PC in LDL. SM is thought to have a higher affinity for cholesterol than PC, arising from the greater hydrogen-bond capacity of SM, due to the hydroxyl group (not present in PC) (*37*−*39*). However, other work has suggested that it is not the intrinsic structural differences of PC and SM that determine the affinity of cholesterol but the composition and chain length of the fatty acyl chains (*31*, *36*, *40*−*44*). Smaby et al. (*44*) found little difference in the condensing effect of cholesterol when the phase state and hydrocarbon chain differences of PC and SM were minimized. Their results also indicated that it was the *sn*-1 position of PC that was critical. These various studies suggest that the strong interaction between cholesterol and SM arises from van der Waals interactions between the steroid ring and the fatty acyl chains; thus the acyl chain composition may be critical in influencing the affinity of cholesterol for SM. Cholesterol has a higher affinity for saturated fatty acyl chains, and in LDL, the majority of SM molecules have saturated (70−75%) fatty acyl chains (*45*). These factors may strongly influence the mobility of SM in LDL.

Modeling the LDL Surface Structure. Approximately 30% or more of the LDL surface is covered by apoB (*46*). Previous data from our laboratory (*17*) suggested that approximately 25−35% of PC headgroups are bound to apoB, although the possibility that a small proportion of SM-apoB interactions exist could not be ruled out. Our results indicate that additional PL interactions also exist. The (free) PC headgroups exhibiting a relatively high mobility (54 ms) may be due to associations with neighboring PL molecules or perhaps weaker interactions with apoB, i.e., those located in fairly close proximity to the apoB protein, although not tight enough to render them virtually immobile on the NMR time scale. As mentioned above, SUVs composed of SM only form condensed bilayers (the headgroups showing low mobility); thus the proportion of SM in LDL that exhibits a low mobility is likely to be due to interactions with neighboring SM (or possibly PC). These conclusions are supported by previous studies carried out in this laboratory (*47*). The T_2 values of the outer layer methyl headgroups in SUVs composed of PC/SM/cholesterol (molar ratio of 1.5:1:1), were fT_{2s}, 0.32; T_{2s}, 25 ms; fT_{2l}, 0.68 and T_{2l}, 87 ms for PC and for SM were fT_{2s}, 0.37; T_{2s}, 26 ms; fT_{2l}, 0.63, and T_{2l}, 81 ms. Since in single PC vesicle systems, PC headgroups are more mobile, it was concluded that the low-mobility PCs were interacting with unesterified cholesterol and the higher mobility PCs were associated with neighboring PLs. This is similar to the situation in LDL, where there is a proportion of PC with low mobility that we suggest is due to interactions with unesterified cholesterol. The interaction of PC headgroups with unesterified cholesterol, depending on the acyl chain composition, is likely to have a condensing effect such that the higher proportion of unsaturated chains in PC compared to SM are restricted in their gauche (kinked) conformations, enabling tighter packing, increasing intermolecular interactions, and decreasing mobility. The more mobile pool of PCs in LDL (54 ms) are not as mobile as those in SUVs, indicating that the presence of apoB may have an overall rigidifying influence, perhaps through the weak interactions postulated above. The mobility of SM in LDL more closely resembled those in SUVs. Approximately 63% of SM in SUVs had a higher mobility (81 ms) and 37% had a low mobility (26 ms), similar to LDL. Since single SM vesicle systems show low mobility and incorporation of cholesterol is thought to act as a spacer increasing headgroup freedom, we concluded that the pool of relatively mobile SM was due to interactions with unesterified cholesterol. The same conclusion was therefore drawn for LDL; the relatively immobile pool of SM was attributed to close packing with neighboring SM (and/or PC), with perhaps weak interactions with apoB, and the (85%) SM molecules, which have a long T_2 component, are due to interactions with unesterified cholesterol. The unesterified cholesterol may interact preferentially with SM, causing a separation of headgroup interactions and enabling more free isotropic rotation. SM molecules with saturated fatty acyl chains may be targeted into specific microdomains at the LDL surface by preferential interaction with unesterified cholesterol, whereas (poly)unsaturated SM molecules, which comprise only 25−30% of SM molecular species (*45*), form separate domains as they preferentially interact with either apoB or other neighboring PL.

The interpretation of these ^{1}H NMR data suggests relatively long-lived weak apoB−PL, cholesterol−PL, and PL−PL interactions observable on the NMR time scale. Our previous studies (*17*) describing strong PL−apoB interactions indicated relatively long-lived complexing of PL headgroups with apoB. It has been suggested by Yeagle (*48*) that, for immobilization of PL headgroups, the protons would have to be complexed to apoB on a time scale $>10^{-3}$ s, while the fatty acyl hydrocarbon chains of the same PL could be moving on and off apoB and from one orientation to another on the protein (or interacting with cholesterol) in the same time scale, making them perhaps harder to detect by NMR.

Recent literature supports a model for LDL in which the distribution and existence of cholesterol-deficient and cholesterol-rich domains at the surface alter the surface order and conformation of apoB. It seems reasonable to suggest that a major factor influencing the formation of microdomains is the interaction of phospholipids with unesterified cholesterol probably dependent on fatty acyl chain composition and the relative proportions of PC and SM. Further studies involving T_2 measurements of phospholipid vesicles and reconstituted LDL, as well as LDL from human volunteers, will be necessary to elucidate the precise nature of the surface interactions of PL, cholesterol, and apoB.

Circulating LDL is composed of several subclasses, which can be subfractionated on the basis of their particle size and density. The current studies were performed on unfractionated LDL and likely describe the surface characteristics of the main subclass found in normolipidemic individuals. It is of course possible that subclasses of LDL exist with differing PL mobilities and that we are observing a weighted average of the PL environments of independent LDL species. Future studies on LDL subclasses might be directed to this question by determining the PL characteristics, for example, of small dense LDL, thought to be particularly atherogenic and at higher concentrations in groups at risk of developing coronary heart disease (*49*).

ACKNOWLEDGMENT

We are grateful to the University of London Intercollegiate Research Service (ULIRS) for NMR facilities, especially Peter Haycock and Harold Toms at the Department of Chemistry, Queen Mary and Westfield College, London, U.K. (600 MHz service). We are also extremely grateful to Dr. M. Ala-Korpela for valuable advice and guidance in Lorentzian line shape analysis of lipoprotein ^{1}H NMR spectra.

REFERENCES

1. Steinberg, D., Parthasarathy, S., Carew, T. E., Khoo, J. C., and Witztum, J. L. (1989) *N. Engl. J. Med. 320* (14), 915−924.
2. Piha, M., Lindstedt, L., and Kovanen, P. T. (1995) *Biochemistry 34* (32), 10120−10129.
3. Schissel, S. L., Tweedie-Hardman, J., Rapp, J. H., Graham, G., Williams, K. J., and Tabas, I. (1996) *J. Clin. Invest. 98* (6), 1455−1464.
4. Nordestgaard, B. G., Wootton, R., and Lewis, B. (1995) *Arterioscler. Thromb. Biol. 15* (4), 534−542.
5. Anber, V., Griffin, B., McConnell, M., Packard, C. J., and Shepherd, J. (1996) *Atherosclerosis 124* (2), 261−271.
6. Auerbach, B. J., Bisgaier, C. L., Wolle, J., and Saxena, U. (1996) *J. Biol. Chem. 271* (3), 1329−1335.
7. Carmena, R., Ascaso, J. F., Camejo, G., Varela, G., Hurt-Camejo, E, Ordovas, J. M., Martines-Valls, J., Bergstom, M., and Wallin, B. (1996) *Atherosclerosis 125* (2), 243−255.
8. Wiklund O., Bondjers, G., Wright, I., and Camejo, G (1996) *Atherosclerosis 119* (1), 57−67.
9. Witztum, J. L., and Steinberg, D. (1991) *J. Clin. Invest. 88* (6), 1785−1792.
10. Palinski, W., Ord, V. A., Plump, A. S., Breslow, J. L., Steinberg, D., and Witztum, J. L. (1994) *Arterioscler. Thromb. 14* (4), 605−616.
11. Ball, R. Y., Stowers, E. C., Burton, J. H., Cary, N. R., Skepper, J. N., and Mitchinson, M. J. (1995) *Atherosclerosis 114* (1), 45−54.
12. Keys, A. (Ed.) (1970) *Circulation 41* (Suppl. I), I1−I211.
13. Ahrens, E. H., Hirsch, J., Insull, W., Tsaltas, T. T., Blomstrand, R. and Peterson, M. L. (1957) *Lancet 1*, 943−953.
14. Soutar, A. (1978) *Nature 273* (5657), 11−12.
15. Hamilton, J. A., and Morrisett, J. D. (1986) *Methods Enzymol. 128A*, 472−515.
16. Bell, J. D., Sadler, P. J., Macleod, A. F., Turner, P. R., and La Ville, A. (1987) *FEBS Lett. 219* (1), 239−243.
17. Murphy, H. C., Ala-Korpela, M. K., White, J. J., Raoof, A., Bell, J. D., Barnard, M. L., Burns, S. P., and Iles, R. A. (1997) *Biochem. Biophys. Res. Commun. 234* (3), 733−737.
18. Friedewald, W. T., Levy, R. I., and Fredrickson, D. S. (1972) *Clin. Chem. 18*, 499−502.
19. Peterson, G. L. (1977) *Anal. Biochem. 83* (2), 346−356.
20. Lowry, O. H., Rosebrough, N., J., Farr, A. L., and Randall, R. J. (1951) *J. Biol. Chem. 193*, 265−275.
21. Van Geet, A. L. (1970) *Anal. Chem. 42* (6), 2287.
22. Press, W. H., Flannery, B. P., Teukolsky, S. A., and Vetterling, W. T. (1988) *Numerical Recipes in C, The Art of Scientific Computing*, Cambridge University Press, New York.
23. Sommer, A., Prenner, E., Gorges, R., Stütz, H., Grillhofer, H., Kostner, G. M., Paltauf, F., and Hermetter, A. (1992) *J. Biol. Chem. 267* (34), 24217−24222.
24. Finer, E. G., Henry, R., Leslie, R. B., and Robertson, R. N. (1975) *Biochim. Biophys. Acta. 380* (2), 320−337.
25. Chana R. S., Treleaven, W. D., Parmar, Y. I., and Cushley, R. J. (1990) *Biochem. Cell. Biol. 68* (1), 189−198.
26. Fenske, D. B., Chana, R. S., Parmar, Y. I., Treleaven, W. D., and Cushley, R. J. (1990) *Biochemistry 29*, 3973−3981.
27. Lund-Katz, S., and Phillips, M. C. (1986) *Biochemistry 25* (7), 1562−1568.
28. Clayden, N. J., and Hesler, B. D. (1992) *J. Magn. Reson. 98*, 271−282.
29. Ibdah, J. A., and Phillips, M. C. (1988) *Biochemistry 27* (18), 7155−7162.
30. Schmidt, C. F., Barenholtz, Y., and Thompson, T. E. (1977) *Biochemistry 16* (12), 2649−2656.
31. Lund-Katz, S., Laboda, H. M., McLean, L. R., and Phillips, M. C. (1988) *Biochemistry 27* (9), 3416−3423.
32. Deckelbaum, R. J., Shipley, G. G., and Small, D. M. (1977) *J. Biol. Chem. 252* (2), 744−754.
33. Huang, C. H. (1977) *Lipids 12* (4), 348−356.
34. Houslay, M. D., and Stanley, K. K. (1994) *Dynamics of biological membranes. Influence on synthesis, structure and function* pp 71−81. John Wiley and Sons Ltd, Chichester, U.K.
35. Yeagle, P. L., Hutton, W. C., Huang, C. and Martin, R. B. (1977) *Biochemistry 16* (20), 4344−4349.
36. McIntosh, T. J., Simon, S. A., Needham, D., and Huang, C. H. (1992) *Biochemistry 31* (7), 2012−2020.
37. Barenholz, Y., and Thompson, T. E. (1980) *Biochim. Biophys. Acta 604* (2), 129−158.
38. Boggs, J. M. (1987) *Biochim. Biophys. Acta 906*(3), 353−404.
39. Sankaram, M. B., and Thompson, T. E. (1990) *Biochemistry 29* (47), 10670−10675.
40. Demel, R. A., Jansen, J. W., Van Dijck, P. W., and Van Deenen, L. L. (1977) *Biochim. Biophys. Acta 465* (1), 1−10.
41. Gronberg, L., Ruan, Z. S., Bittman, R., and Slotte, J. P. (1991) *Biochemistry 30* (44), 10746−10754.
42. Calhoun, W. I., and Shipley, G. G. (1979) *Biochemistry 18* (9), 1717−1722.
43. Lange, Y., D'Alessandro, J. S., and Small, D. M. (1979) *Biochim. Biophys. Acta 556* (3), 388−398.
44. Smaby, J. M., Brockman, H. L., and Brown, R. E. (1994) *Biochemistry 33* (31), 9135−9142.
45. Myher, J. J., Kuksis, A., Shepherd, J., Packard, C. J., Morrisett, J. D., Taunton, O. D., and Gotto, A. M. (1981) *Biochim. Biophys. Acta 666*(1), 110−119.
46. Schumaker, V. N., Phillips, M. L., and Chatterton, J. E. (1994) *Adv. Protein Chem. 45*, 205−248.
47. Murphy, H. C., Raoof, A., White, J. J., Ala-Korpela, M. K., Barnard, M. L., Bell, J. D., and Iles, R. A. (1997) *Biochem. Soc. Trans. 25*, 22S.
48. Yeagle, P. (1982) *Biophys. J. 37*, 227−239.
49. Griffin, B. A. (1995) *Baill. Clin. Endocrinol. Metab. 9* (4), 687−703.

BI0000115